

# Long-Range Interaction between Charge and Spin Qubits in Quantum Dots

Marcel Serina, Luka Trifunovic, Christoph Kloeffel, and Daniel Loss

*Department of Physics, University of Basel, Klingelbergstrasse 82, CH-4056 Basel, Switzerland*

(Dated: January 15, 2016)

We analyze and give estimates for the long-distance coupling via floating metallic gates between different types of spin qubits in quantum dots made of different commonly used materials. In particular, we consider the hybrid, the singlet-triplet, and the spin-1/2 qubits, and the pairwise coupling between each type of these qubits with another hybrid qubit in GaAs, InAs, Si, and Si<sub>0.9</sub>Ge<sub>0.1</sub>. We show that hybrid qubits can be capacitively coupled strongly enough to implement two-qubit gates, as long as the dimensions of the dots and their distance from the metallic gates are small enough. Thus, hybrid qubits are good candidates for scalable implementations of quantum computing in semiconducting nanostructures.

PACS numbers: 03.67.Lx, 73.21.La, 73.23.Hk

## I. INTRODUCTION

One of the most promising ways to implement the concept of quantum computation<sup>1</sup> is to use the spins of electrons in quantum dots as qubits<sup>2</sup>. Quantum dots fabricated in semiconductor nanostructures are used to confine electrons, which can then be manipulated and measured by electrical gates<sup>3</sup>. Many generalizations of qubits in quantum dots have been proposed and explored over the years<sup>4</sup>. A recent interesting addition is a proposal for a hybrid qubit formed in a double quantum dot by different states of three electrons, where both charge and spin degrees of freedom of the electrons play a role<sup>5-7</sup>. Since all types of spin qubits have their specific weaknesses and strengths, it is useful to ask if one can combine various types of such qubits to make optimal use of their particular advantages.

Furthermore, to successfully implement quantum computation, scalable architectures consisting of many qubits are needed. One of the possibilities to achieve such a goal is to couple the qubits in quantum dots over a long distance by using a metallic floating gate<sup>8</sup>. In this proposal, quantum dots could be hundreds of micrometers apart from each other, coupled in a similar way as electronic components are coupled by wires.

Here, we study a mechanism for entangling various types of spin qubits of distant quantum dots via floating metallic gates and spin-orbit interaction (SOI). This will then allow one to couple hybrid qubits not only among themselves but also with other types of spin qubits. The actual system we consider is composed of two double quantum dots (DQDs)<sup>3,4,9-11</sup>, which are not tunnel coupled to each other. The number of electrons in each DQD can be controlled by tuning the chemical potential via nearby gates. Moreover, the electrons can be moved from the left to the right dot within each DQD by applying a strong bias to it. Thus, full control over the DQD is possible by purely electrical means. The DQDs are separated by a large distance compared to their own size, so that they can only interact capacitively<sup>12</sup>, i.e., via the repulsive Coulomb interaction. This interaction can be enhanced by using a ‘classical’ electromagnetic cavity,

i.e., a metallic gate suspended over the two DQDs, or a floating gate<sup>8</sup>. The strength of the coupling mediated by this gate strongly depends on its geometry, as well as on the position of the DQDs underneath the gate.

There are three different qubit combinations we consider. First, we study the case of two hybrid (H) qubits<sup>5,13</sup>. In the second case, one DQD contains two and the other DQD three electrons, i.e., one DQD hosts a singlet-triplet (ST) qubit<sup>9,14,15</sup> and the other one a hybrid qubit. In these two cases, the SOI is not required, since the coupling can be induced solely by the Coulomb interaction and the Pauli exclusion principle. In the third case, we study a hybrid system where one of the DQDs is singly occupied forming the spin-1/2 (LD) qubit and the second one is triply occupied, i.e., a hybrid qubit. We thus expect an interaction between the LD qubit (single electron) and the hybrid qubit (three electrons) mediated by the floating gate.

Each of these cases will be studied separately. However, it is important to mention that experimentally it is possible to realize the different schemes within the very same experimental setup by only modifying the voltages on the gates.

The paper is organized as follows. First in Sec. II we focus on the H-H and H-ST qubit couplings in GaAs. Then, in Sec. III we calculate H-LD qubit coupling in GaAs and compare all the couplings in the four different semiconducting materials commonly used for the fabrication of quantum dots, namely GaAs, InAs, Si, and Si<sub>0.9</sub>Ge<sub>0.1</sub>. Finally, in Sec. IV we summarize and give some conclusions.

## II. H-H AND H-ST COUPLING

The DQD H-qubit, introduced recently in Ref. 5, operates on three different three-electron-states<sup>16</sup> as illustrated in Fig. 1. In order to implement a universal set of quantum gates, one must be able to couple such qubits to each other pairwise<sup>17</sup>.

The idea pursued here is to couple two such H-qubits over a (possibly long) distance via a floating gate in the

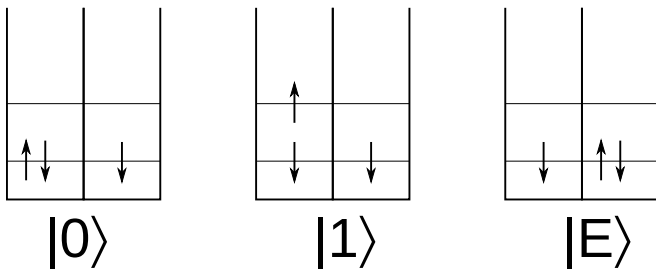


Figure 1. States of the double dot hybrid qubit. The logical states of the hybrid qubit are defined as follows:  $|0\rangle = |S\rangle |\downarrow\rangle$ , where  $|S\rangle$  denotes the singlet of the two electrons in the ground state of the first dot and  $|\downarrow\rangle$  denotes the electron with the spin down in the second dot, and  $|1\rangle = |T_0\rangle |\downarrow\rangle$ , where  $|T_0\rangle$  denotes the triplet state of the two electrons with zero projection of spin along the quantization axis. The state  $|E\rangle = |\downarrow\rangle |S\rangle$  is used as an intermediate state to prepare the logical states.

way proposed in Ref. 8 and to estimate the strength of the resulting coupling between them. This setup is promising due to its simplicity and scalability and provides a pathway for implementing large-scale quantum computing architectures. The coupling is mediated through the Coulomb interaction of the induced charges on the floating gate caused by the charge distributions in the qubits. As the different states of the hybrid qubit have different charge distributions (in contrast to qubits based on the states of a single quantum dot), it is sufficient to take into account the Coulomb interaction in order to estimate the coupling. Thus, one may assume that the hybrid qubit is a charge qubit and may disregard the spin degrees of freedom (which are on the other hand important for the noise and decoherence description).

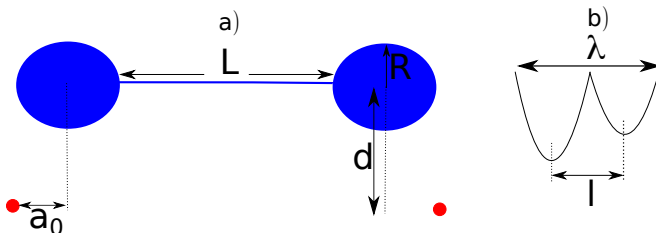


Figure 2. a) Setup consisting of a floating metallic gate (blue) and two DQDs (red dots). b) Sketch of the confinement potential of a DQD as function of separation of minima. Here,  $a_0$  is an in-plane distance between the floating gate disc center and the DQD,  $d$  is the vertical distance between the floating gate disc center and the DQD,  $R$  is the radius of the floating gate disc,  $L$  is the length of the section connecting the discs,  $R_W$  is the radius of this section (modelled as wire),  $\lambda$  is the length of the DQD and  $l$  is the distance between the DQD minima.

Following Ref. 8, we now describe the setup analytically. The induced charge (in units of  $e$ ) on the disc of the floating gate due to an electron at position  $\mathbf{r}$  is given

by

$$q_{ind}(\mathbf{r}) = \frac{2}{\pi} \arcsin(R/\xi_{\mathbf{r}}), \quad (1)$$

where  $R$  is the radius of the disc and  $a_0$  is the distance between the DQD and the ellipsoid center (see Fig. 2). The ellipsoidal coordinate  $\xi_{\mathbf{r}}$  is given by

$$2\xi_{\mathbf{r}}^2 = R^2 + d^2 + |\mathbf{a}_0 + \mathbf{r}|^2 + \sqrt{(R^2 + d^2 + |\mathbf{a}_0 + \mathbf{r}|^2)^2 - 4R^2|\mathbf{a}_0 + \mathbf{r}|^2}. \quad (2)$$

From the electrostatic potential of the charged thin disc we arrive at the following expression for the coupling potential<sup>18</sup>,

$$V(\mathbf{r}_1, \mathbf{r}_2) = \frac{\pi\alpha_q e^2 q_{ind}(\mathbf{r}_1) q_{ind}(\mathbf{r}_2)}{\kappa R}, \quad (3)$$

where  $\kappa = 4\pi\epsilon_0\epsilon_r$  is the dielectric constant,  $\alpha_q = \frac{C_d}{C_w + 2C_d}$  is the charge distribution factor of the gate and  $C_d$  and  $C_w$  are the capacitances of the metal discs and connecting metal wire, respectively. In order to obtain an estimate of the interaction we need to model the charge distributions in the different logical states. Electrons in the DQDs are trapped inside the two overlapping two-dimensional (2D) parabolic potential wells (see Fig. 2b), thus their orbital states in each quantum dot are in good approximation the same as the eigenstates of the 2D simple harmonic oscillator (SHO)<sup>19</sup>. The charge distributions in these states are equivalent to the probability densities of the corresponding SHO states. The probability density in the ground state is Gaussian and in the first excited state we have two disjoint peaks shifted with respect to the center of the well to both sides by  $b = \sqrt{\frac{\hbar}{m^*\omega}}$ , where  $\hbar\omega$  is the single-particle level spacing in the quantum dot, and  $m^*$  is the effective mass of the electron. We define  $\lambda = l + 2b$  as the length of the DQD, where  $l$  is the distance between the minima of the potential (see Fig. 2b). Using a model with 2D continuous charge distributions in the plane of two-dimensional electron gas (2DEG) we obtain the following expression for the coupling of the two states  $i, j$  with charge densities  $\rho_i(\mathbf{r}), \rho_j(\mathbf{r})$ ,

$$V_{ij} = \frac{\pi\alpha_q e^2}{\kappa R} \times \int d^2\mathbf{r}_1 \int d^2\mathbf{r}_2 q_{ind}(\mathbf{r}_1) q_{ind}(\mathbf{r}_2) \rho_i(\mathbf{r}_1) \rho_j(\mathbf{r}_2). \quad (4)$$

The four-dimensional integrals can be evaluated numerically. However, in order to gain more insight we evaluate the matrix elements in Eq. (4) first analytically by adopting the following approximations. We model the Gaussian wave functions by delta functions, thus considering the interaction of point charges. Considering furthermore, that the DQDs are positioned such that one minimum is below the edge of the discs, our assumptions are illustrated in Fig. 3.

Now we are prepared to calculate the matrix elements of the potential  $V$  between the different states of two

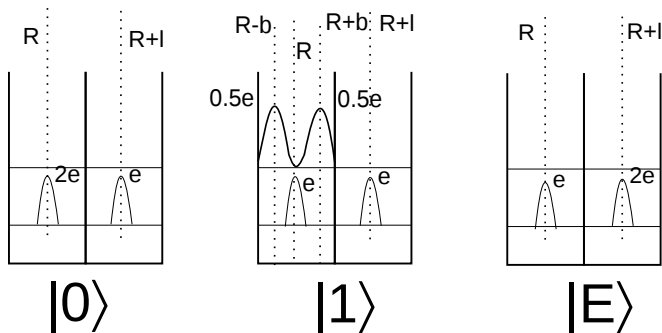


Figure 3. Charge distributions in the logical states of the DQD forming the hybrid qubit. In the point charge approximation we model the charge distribution via delta functions localized at the distances shown by dotted lines, with the corresponding charges in units of the elementary charge. In the numerical integration we use for the charge distributions the corresponding eigenfunctions of the parabolic potential.

DQDs. As the Coulomb interaction does not include the spins, spins of the states are always conserved. Thus, because the logical states are orthogonal in spin space, we get (where  $i, j, k, l = 0, 1, E$ )

$$\langle i, j | V | k, l \rangle = \delta_{ik} \delta_{jl} V_{kl}. \quad (5)$$

As an example we can write the expression for one of the matrix elements in the point charge approximation as follows

$$\begin{aligned} \langle 0, 1 | V | 0, 1 \rangle &= V(R-b, R) + \frac{1}{2} V(R-b, R+l) \\ &+ V(R+b, R) + \frac{1}{2} V(R+b, R+l) \\ &+ 2V(R, R) + V(R, R+l) \\ &+ 2V(R+l, R) + V(R+l, R+l), \end{aligned} \quad (6)$$

where  $V(x_1, x_2)$  denotes the Coulomb interaction of two point charges placed at the positions  $x_1, x_2$ . The charge in the hybrid qubit is equal to three elementary charges, thus the sum of the prefactors of all terms in Eq. (6) must be nine.

We fix the parameters of the setup as follows. For the spatial dimensions of the DQDs we assume the typical values  $\lambda = 250\text{nm}$ ,  $l = 150\text{nm}$ ,  $d = 100\text{nm}$ ,  $R = 4d$ , and  $a_0 = 4d$ ,  $L = 10\mu\text{m}$ ,  $R_W = 30\text{nm}$  while  $\alpha_q = 0.19$  and  $\hbar\omega = 0.5\text{meV}$  (in GaAs) similar to the values in Ref. 8.

Now we can choose any of the two logical states and write their interaction energies in the form of a  $4 \times 4$  matrix. For example, we choose the states  $|0\rangle, |1\rangle$  and then write the projection of  $V$  onto this subspace as

$$V = \text{diag}(V_{00}, V_{01}, V_{01}, V_{11}), \quad (7)$$

where we used  $V_{01} = V_{10}$ . We can construct a two-qubit gate that is equivalent to the CNOT gate up to single-qubit operations as follows<sup>20</sup>

$$\mathcal{H} = C\sigma_1^z\sigma_2^z, \quad (8)$$

$$\exp\left(i\mathcal{H}\frac{\pi}{4C}\right) = e^{i\frac{\pi}{4}} \begin{pmatrix} 1 & 0 & 0 & 0 \\ 0 & -i & 0 & 0 \\ 0 & 0 & -i & 0 \\ 0 & 0 & 0 & 1 \end{pmatrix}. \quad (9)$$

To implement a quantum gate we decompose the interaction into a tensor product of Pauli matrices and get

$$\begin{aligned} V &= \frac{V_{00} + V_{11} + 2V_{01}}{4} + \frac{V_{00} - V_{11}}{4}\sigma_2^z \\ &+ \frac{V_{00} - V_{11}}{4}\sigma_1^z + \frac{V_{00} + V_{11} - 2V_{01}}{4}\sigma_1^z\sigma_2^z. \end{aligned} \quad (10)$$

The last term in this decomposition enables us to implement the CNOT gate<sup>2</sup>, so we obtain the qubit-qubit coupling  $C \equiv (V_{00} + V_{11} - 2V_{01})/4 = 3.9 \times 10^{-10}\text{eV}$  from the point charge approximation, while  $C = 5.1 \times 10^{-10}\text{eV}$  from the continuous charge distributions. Since these results are very similar, we conclude that the numerical integration is well reproduced by the point charge approximation. One can significantly increase the coupling by varying the setup parameters. The coupling is most significantly dependent on the vertical distance of the gate and the DQD parameter  $d$ . Assuming that  $d = 10\text{nm}$  can be realized, we are able to obtain a coupling strength of  $C = 1\mu\text{eV}$  (see below in Sec. III).

Next we study the interaction of the ST qubit, *i.e.*, singlet-triplet states of the two electrons in the DQD, and the hybrid qubit, *i.e.*, three electrons in the DQD with states 0,1, and  $E$ , see Fig. 3. We assume the DQD for the ST qubit to be in the strongly detuned regime, thus the singlet state is effectively a (2,0) charge state and the triplet state is effectively a (1,1) charge state (only ground states of the dots forming DQDs can be occupied). Then we are able to calculate the matrix elements, for instance  $\langle S, 1 | V | S, 1 \rangle \equiv V_{S1}$ , with

$$V_{S1} = 2V(R, R) + V(R-b, R) + V(R+b, R) + 2V(R, R+l). \quad (11)$$

We obtain the ZZ coupling  $C = 1.1 \times 10^{-8}\text{eV}$  for the point charges and  $C = 2.7 \times 10^{-8}\text{eV}$  for the continuous charge distributions. As a check of the numerics we calculate the ST-ST coupling by the continuous distributions as well and compare it to the expected value of  $10^{-5} - 10^{-6}\text{eV}$  obtained from Ref. 8. We get  $c_{ST-ST} = 1.5\mu\text{eV}$ .

It is then interesting to ask why the obtained H-H and H-ST couplings are much smaller than the ST-ST. When we look at the logical states of the hybrid qubit, we can see that the charge distribution in the second quantum dot is the same in both logical states, thus this interaction gives us no contribution to the coupling, in contrast to the states of the ST qubit. Moreover, the charge difference between the singlet and the triplet states in the single dot is small,  $\delta q = 4.7 \times 10^{-5}e$  according to the calculations in Ref. 21, in contrast to the charge difference

between the singlet and triplet states in the ST qubit where  $\delta q = 2.7 \times 10^{-2}e$ .

It is worth mentioning that when we use the state  $|E\rangle$  instead of the state  $|1\rangle$  as a computational basis for the hybrid qubit, we obtain much larger couplings due to the different charge configurations in both wells in the different logical states. For H-H and H-ST we get about the same coupling strengths,  $c_{H-H} \approx c_{H-ST} \approx 0.3\mu\text{eV}$ , which is on the order of what one would expect for the Coulomb interaction.

### III. H-LD COUPLING

In this section we want to evaluate the coupling between the hybrid or the ST qubit with the LD qubit in a single quantum dot (logical states  $|\uparrow\rangle$  and  $|\downarrow\rangle$ ). Because of the same charge distributions in the states of the LD qubit, we now need to include the SOI in order to lift this degeneracy. We adopt a perturbative approach, as the SOI is at least two orders of magnitude weaker than the Coulomb interaction.

First we would like to get a simple estimate of the coupling strengths. We can use the estimates from Ref. 8 for the ST-LD coupling, since the coupling mechanism in this case is also given by the SOI-induced difference in the LD qubit charge densities. We find  $c_{H-LD} \sim \frac{E_Z \alpha}{b\omega^2 \hbar}$ , where  $E_Z = g\mu_B B$  is the Zeeman energy,  $\alpha$  is the Rashba SOI coupling,  $b = \sqrt{\frac{\hbar}{m^* \omega}}$ , and when we use  $E_Z = 0.5\hbar\omega$  and  $\lambda_{SO} = \frac{\hbar}{m^* \alpha} = 2\mu\text{m}$ , this yields an estimate  $c_{H-LD} = 10^{-10} - 10^{-9}\text{eV}$ . Assuming the magnetic field perpendicular to the 2DEG we get a  $\sigma_1^x \sigma_2^z$  coupling (we assume the simplest possible geometry, in general we get  $\sigma_1^y \sigma_2^z$  as well and the weights of the two coupling terms are given by trigonometric functions).

We proceed with a perturbative approach. First, we use quasi-degenerate perturbation theory (Löwdin partitioning) according to Ref. 22. Our aim is to obtain the correction to the charge densities in the LD qubit when we include the SOI in the first order in the corresponding quantum dot. The Hamiltonian of the single quantum dot reads

$$\mathcal{H}_{LD} = H_0 + H_{SOI} = \frac{p_x^2 + p_y^2}{2m^*} + \frac{1}{2}m^*(x^2 + y^2)\omega^2 + \frac{g}{2}\mu_B \sigma^z + \alpha(p_x \sigma^y - p_y \sigma^x), \quad (12)$$

where for simplicity we included only the Rashba SOI term. In this approach we are able to decouple the two subspaces of the full Hamiltonian  $\mathcal{H}_{LD}$  (in our case the subspace is spanned by the two degenerate ground states of  $H_0$ ,  $|\psi_\sigma^0\rangle$  and the first two excited states with the same energy  $|\psi_\sigma^x\rangle$  and  $|\psi_\sigma^y\rangle$ , where  $\sigma = \uparrow, \downarrow$  is a spin index), thus removing the terms in the full  $\mathcal{H}_{LD}$  between these two subspaces in the first order in SOI by means of the unitary transformation  $\tilde{\mathcal{H}}_{LD} = e^{-S}\mathcal{H}_{LD}e^S$ . With the known transformation of the full Hamiltonian, the states

are transformed as follows (in the first order in the SOI)  $|\tilde{\phi}\rangle = S|\phi\rangle$ , which gives us

$$|\tilde{\psi}_\uparrow^0\rangle = |\psi_\uparrow^0\rangle - S_1|\psi_\uparrow^x\rangle - S_2|\psi_\uparrow^y\rangle, \quad (13)$$

$$S_1 = \frac{\hbar}{-\hbar\omega + E_Z} \frac{\alpha}{2b}, \quad (14)$$

$$S_2 = \frac{\hbar}{-\hbar\omega + E_Z} \frac{i\alpha}{2b}, \quad (15)$$

$$|\tilde{\psi}_\downarrow^0\rangle = |\psi_\downarrow^0\rangle - S_3|\psi_\downarrow^x\rangle - S_4|\psi_\downarrow^y\rangle, \quad (16)$$

$$S_3 = \frac{\hbar}{-\hbar\omega - E_Z} \frac{-\alpha}{2b}, \quad (17)$$

$$S_4 = \frac{\hbar}{-\hbar\omega - E_Z} \frac{i\alpha}{2b}. \quad (18)$$

After this transformation, the states of the LD qubit have different charge distributions and we can calculate the matrix elements of the Coulomb coupling between the hybrid qubit and the LD qubit in the basis  $\{|0\uparrow\rangle, |0\downarrow\rangle, |1\uparrow\rangle, |1\downarrow\rangle\}$  and find

$$V = \begin{pmatrix} a & V_0 & 0 & 0 \\ V_0 & c & 0 & 0 \\ 0 & 0 & a & V_1 \\ 0 & 0 & V_1 & c \end{pmatrix}, \quad (19)$$

where  $V_0, V_1, a, c$  are corresponding matrix elements in the basis mentioned. Then we obtain the coupling  $V = \frac{V_0 - V_1}{2} \sigma_1^x \sigma_2^z \equiv c_{H-LD} \sigma_1^x \sigma_2^z$ . The diagonal terms give no qubit-qubit coupling because they exactly cancel in the  $\sigma_1^z \sigma_2^z$  term. We obtain  $c_{H-LD} = 1.9 \times 10^{-10}\text{eV}$ , which is in agreement with our naive estimates. The coupling is a rather complicated function of the two four-dimensional integrals like Eq. (4), but the dependence on the setup parameters is in the  $S_i$  coefficients. Assuming  $\hbar\omega \gg E_Z$ , we can use an expansion  $\frac{1}{-\hbar\omega + E_Z} \approx -\frac{\hbar\omega + E_Z}{(\hbar\omega)^2}$  and as the coupling is proportional to the difference of the  $S_i$  coefficients, only the Zeeman part from the expansions contributes (this is the remnant of the van Vleck cancellation), and the coupling then has the dependence  $c_{H-LD} \sim \frac{E_Z \alpha}{2b\omega^2 \hbar}$ , which is the form we expected from our naive estimation.

The last approach we exploit for the perturbation theory is the Schrieffer-Wolff (SW) transformation. The idea is identical with the previously used Löwdin partitioning, but now we are able to decouple the ground state of the SHO from all the excited states (it is an important improvement, because of the constant energy spacing between the states of the SHO) and therefore obtain the most precise estimate. In this paper we use the same terminology as in the cited references, thus decoupling of the ground state from the first excited state we call Löwdin partitioning as in Ref. 22 and decoupling from all the excited states we call SW transformation as in Ref. 23. The SW transformation involves calculation of the inverse Liouville operator, which can be done exactly for the SHO Hamiltonian according to Ref. 23. The SW transformation yields the change of the charge distribution in the single quantum dot due to the SOI in the first

order as<sup>23</sup>

$$\delta\rho(\mathbf{r}) = \frac{2E_Z\alpha}{b^2\omega^2\hbar}\rho_0(x\sigma^x + y\sigma^y), \quad (20)$$

where  $\rho_0$  is the charge distribution in the ground state of the SHO, written as a charge density operator respecting the spin structure. For the change of the states, this results in<sup>24</sup>

$$|\tilde{\psi}_\uparrow^0\rangle = |\psi_\uparrow^0\rangle + S|\psi_\uparrow^x\rangle - iS|\psi_\downarrow^y\rangle, \quad (21)$$

$$|\tilde{\psi}_\downarrow^0\rangle = |\psi_\downarrow^0\rangle + S|\psi_\uparrow^x\rangle + iS|\psi_\downarrow^y\rangle, \quad (22)$$

$$S = \frac{E_Z\alpha}{b\omega^2\hbar}. \quad (23)$$

From the calculation of the matrix elements of the Coulomb interaction we get the same form as in Eq. (19) and obtain the coupling  $c_{H-LD} = 2.9 \times 10^{-10}$  eV. Again, as can be seen from Eq. (20), we obtain the initially expected dependence on the setup parameters. This analysis has verified our numerical calculations, so from now on we use the numerical integration to get the H-H and H-ST coupling and the numerical integration together with the SW transformation for the H-LD coupling.

We can also obtain a two orders of magnitude stronger coupling by using a quantum dot material with stronger SOI (like InAs). To verify these assumptions, we calculated the couplings for the fixed setup parameters mentioned before for different materials, with the following material parameters: for GaAs<sup>8</sup>  $\lambda_{SO} = 2.0 \times 10^{-6}$  m,  $m^* = 0.067m_e$ ,  $\hbar\omega = 0.5$  meV,  $\epsilon_r = 13$ , for InAs<sup>25</sup>  $\lambda_{SO} = 1.64 \times 10^{-7}$  m,  $m^* = 0.023m_e$ ,  $\hbar\omega = 1.3$  meV,  $\epsilon_r = 15.15$ , in Si<sup>26</sup>  $\lambda_{SO} = 2.6 \times 10^{-5}$  m,  $m^* = 0.26m_e$ ,  $\hbar\omega = 0.1$  meV,  $\epsilon_r = 11.7$ , and for Si<sub>0.9</sub>Ge<sub>0.1</sub><sup>27</sup>  $\lambda_{SO} = 2 \times 10^{-5}$  m,  $m^* = 0.19m_e$ ,  $\hbar\omega = 0.2$  meV,  $\epsilon_r = 12.2$ .  $E_Z = 0.5\hbar\omega$  so it also varies in each 2DEG. We have chosen  $\omega$  in every 2DEG such that it is experimentally well accessible and keeps  $b$  close to 50nm. The results are listed in Table I. However, the couplings for this setup are rather small. If we want to further enhance them, we need to consider smaller geometries, and the simplest way is to shorten the distance  $d$  and then the radius  $R$  and the position of the dot  $a_0$ , what results in small decrease of  $\alpha$ . As expected, the couplings are most strongly dependent on the vertical distance  $d$  between the dots and the metallic gate. To quantify this dependence, we calculated the couplings again for two smaller setups. In Table II, we present the results for currently feasible fabrication parameters with  $d = 57$  nm,  $\alpha_q = 0.13$  and  $R = a_0 = 228$  nm, and in Table III for  $d = 10$  nm,  $\alpha_q = 0.03$  and  $R = a_0 = 40$  nm to demonstrate the strong dependence on  $d$ . Parameters of the DQD  $\lambda = 250$  nm and  $l = 150$  nm are fixed. As was shown in Ref. 8, when the influence of the surrounding gates is included into the calculation of the couplings, we obtain another two orders of magnitude increase, which makes the hybrid qubit a very promising platform for quantum computation.

To enhance the relatively small coupling in the H-LD case in Si and in Si<sub>0.9</sub>Ge<sub>0.1</sub> one can include the micro-magnet into the setup of DQDs as was proposed in Ref. 28. In 1D wire<sup>29</sup> with Rashba SOI and Zeeman coupling, one can gauge away the SOI, what results in helical Zeeman coupling

$$H_Z = \frac{Bg\mu}{2} \left( \hat{\mathbf{z}} \cos\left(\frac{2x}{\lambda_{SO}}\right) + \hat{\mathbf{y}} \sin\left(\frac{2x}{\lambda_{SO}}\right) \right). \quad (24)$$

Here  $\hat{\mathbf{y}}$  and  $\hat{\mathbf{z}}$  are directions in spin space and  $x$  corresponds to the coordinate along the DQD axis. Because the DQD length  $\lambda = 250$  nm is much smaller than  $\lambda_{SO} = 2.6 \times 10^{-5}$  m in Si, one can expand the trigonometric functions in the small parameter  $\frac{2x}{\lambda_{SO}}$  and that gives homogeneous magnetic field gradient in the  $x$  direction. This justifies the formula<sup>28</sup>

$$b_{\text{tot}} = 2B \left( \frac{\alpha}{\hbar m^*} + \frac{b_{\text{MM}}}{2B} \right), \quad (25)$$

where  $b_{\text{tot}}$  is the total magnetic field gradient and  $b_{\text{MM}}$  is the magnetic field gradient from the micro-magnet. Therefore, one can include the magnetic field gradient from the micro-magnet as an effective SOI. For the best micro-magnets we have  $b_{\text{MM}}$  up to 1T/ $\mu\text{m}$  and that gives the effective SOI strength in Si induced by micro-magnet as high as  $\lambda_{SO} = 2 \times 10^{-6}$  m and the same holds in the case of Si<sub>0.9</sub>Ge<sub>0.1</sub>. In total, this would enhance all the H-LD couplings in Si and Si<sub>0.9</sub>Ge<sub>0.1</sub> by one order of magnitude.

For a comparison of the H-H and H-ST couplings it is important to keep in mind that the materials differ from each other only in the relative permeabilities and effective masses in the context of this calculation. Choosing different values of  $\omega$  for different 2DEGs to keep the  $b$  approximately constant we effectively almost get rid of the dependence on the effective mass, thus small differences remaining among the 2DEGs in H-H and H-ST are caused only by small variations in  $b$  and relative permittivity.

As anticipated, strong SOI is needed for implementing the H-LD coupling, which favours InAs as the choice of material for the quantum dots.

In our analysis of charge distributions in the states of the DQD, we assumed that all the excited states have an excited orbital part. In Si we therefore assume, that the orbital level spacing  $\hbar\omega = 0.1$  meV is smaller than the valley splitting. As was shown<sup>30</sup>, it is possible to tune the valley splitting in the range of 0.3-0.8 meV. Moreover, it is possible to fabricate<sup>31</sup> the dots with valley splitting up to 10 meV and that is clearly sufficient to be sure that the excitation originates from the orbital part. Based on that, it should be possible to have Si DQDs with the sufficiently large valley splittings.

At the end of this section, we would like to summarize the dependence of the couplings on the sample parameters. For the H-H and H-ST coupling, we can conclude for the scaling from Eqs. (1)-(3) that  $c \sim \frac{1}{d^2}, \frac{1}{R}, \frac{1}{b}$ , and moreover for the H-LD coupling from Eq. (19) that  $c \sim B, \alpha$ .

Coupling [ $\mu\text{eV}$ ]	InAs	GaAs	$\text{Si}_{0.9}\text{Ge}_{0.1}$	Si
H-H	$5.5 \times 10^{-4}$	$5.1 \times 10^{-4}$	$4.3 \times 10^{-4}$	$9.3 \times 10^{-4}$
H-ST	$2.6 \times 10^{-2}$	$2.7 \times 10^{-2}$	$2.6 \times 10^{-2}$	$3.8 \times 10^{-2}$
H-LD	$3.8 \times 10^{-3}$	$2.9 \times 10^{-4}$	$2.4 \times 10^{-5}$	$4.0 \times 10^{-5}$

Table I. Calculated strengths of the coupling between the three different types of qubits [spin-1/2 (LD), singlet-triplet (ST), and hybrid (H) qubit] in DQDs for  $d = 100\text{nm}$ ,  $\alpha_q = 0.19$ ,  $R = a_0 = 400\text{nm}$  (see Fig. 2) for four different semiconducting materials commonly used for the realization of DQDs.

Coupling [ $\mu\text{eV}$ ]	InAs	GaAs	$\text{Si}_{0.9}\text{Ge}_{0.1}$	Si
H-H	$5.3 \times 10^{-3}$	$5.1 \times 10^{-3}$	$4.3 \times 10^{-3}$	$8.9 \times 10^{-3}$
H-ST	$1.3 \times 10^{-1}$	$1.4 \times 10^{-1}$	$1.3 \times 10^{-1}$	$1.9 \times 10^{-1}$
H-LD	$2.1 \times 10^{-2}$	$1.6 \times 10^{-3}$	$1.4 \times 10^{-4}$	$2.2 \times 10^{-4}$

Table II. Same as in Table I for  $d = 57\text{nm}$ ,  $\alpha_q = 0.13$  and  $R = a_0 = 228\text{nm}$ .

Coupling [ $\mu\text{eV}$ ]	InAs	GaAs	$\text{Si}_{0.9}\text{Ge}_{0.1}$	Si
H-H	$6.6 \times 10^{-1}$	$7.4 \times 10^{-1}$	$7.4 \times 10^{-1}$	$8.8 \times 10^{-1}$
H-ST	2.5	3.0	3.2	3.0
H-LD	$3.2 \times 10^{-2}$	$5.8 \times 10^{-3}$	$9.2 \times 10^{-4}$	$4.4 \times 10^{-5}$

Table III. Same as in Table I for  $d = 10\text{nm}$ ,  $\alpha_q = 0.03$  and  $R = a_0 = 40\text{nm}$ .

#### IV. CONCLUSIONS

We have studied an experimentally realizable setup which allows different types of qubits in DQDs to be coupled among themselves and between them. In particular, we have shown that using a metallic floating gate, it is possible to capacitively couple the hybrid qubit to a single spin 1/2, to singlet-triplet qubit, or to another hybrid qubit. First we employed a simple approximation, where the charge density within the quantum dot is treated as a point charge distribution and calculated the couplings between the two hybrid qubits as well as between the ST and the hybrid qubit. Furthermore, we have verified the point charge approximation using the numerical integration of the Gaussian charge distribution within each quantum dot. Then, we have calculated perturbatively the coupling between the LD and the hybrid qubit via the charge differences induced by a weak Rashba SOI. To investigate further the influence of the material used to fabricate quantum dots and the geometries of the setup, we have calculated the couplings for three different sizes of the structure, and for the four different semiconducting materials GaAs, InAs, Si, and  $\text{Si}_{0.9}\text{Ge}_{0.1}$ .

We have discussed the influence of the strength of the Rashba SOI on the H-LD coupling, leading to the

anticipated result that for this coupling the most suitable material is InAs, due to the largest Rashba coupling constant. To increase the strength of the H-H coupling we can propose several possibilities. With the currently achievable sizes of about  $d = 57\text{nm}$  using one of the 2DEGs mentioned and assuming that including the whole sample geometry with the surrounding gates can give us another two orders of magnitude as calculated in Ref. 8, we are able to reach the  $\mu\text{eV}$  coupling regime. This amounts to very fast gate operation times on the order of tens of picoseconds. On the other hand, InAs and GaAs are not nuclear spin free in contrast to Si (which can be isotopically purified), which are thus less favorable in terms of the  $T_2^*$  dephasing time. Assuming that fabrication down to  $d = 10\text{nm}$  is feasible, one can expect that  $\mu\text{eV}$  couplings can be realized with Si dots as well, which will make Si hybrid qubits a promising platform for quantum-dot-based quantum information processing and quantum computation.

#### ACKNOWLEDGMENTS

We are especially grateful to M. A. Eriksson for interesting us in this problem and for useful comments. This work was supported in part by the Swiss NF, NCCR QSIT, SiSPIN, and IARPA.

<sup>1</sup> R. Feynman, International Journal of Theoretical Physics **21**, 467 (1982)

<sup>2</sup> D. Loss and D. P. DiVincenzo, Phys. Rev. A **57**, 120 (1998)

- <sup>3</sup> W. G. van der Wiel, S. De Franceschi, J. M. Elzerman, T. Fujisawa, S. Tarucha, and L. P. Kouwenhoven, *Rev. Mod. Phys.* **75**, 1 (2002)
- <sup>4</sup> C. Kloeffel and D. Loss, *Annual Review of Condensed Matter Physics* **4**, 51 (2013)
- <sup>5</sup> T. S. Koh, J. K. Gamble, M. Friesen, M. A. Eriksson, and S. N. Coppersmith, *Phys. Rev. Lett.* **109**, 250503 (2012)
- <sup>6</sup> D. Kim, D. R. Ward, C. B. Simmons, J. K. Gamble, R. Blume-Kohout, E. Nielsen, D. E. Savage, M. G. Lagally, M. Friesen, S. N. Coppersmith, and M. A. Eriksson, *Nat. Nano.* **10**, 243 (2015)
- <sup>7</sup> D. Kim, D. R. Ward, C. B. Simmons, D. E. Savage, M. G. Lagally, M. Friesen, S. N. Coppersmith, and M. A. Eriksson, *Npj Quant. Inf.* **1** (2015)
- <sup>8</sup> L. Trifunovic, O. Dial, M. Trif, J. R. Wootton, R. Abebe, A. Yacoby, and D. Loss, *Phys. Rev. X* **2**, 011006 (2012)
- <sup>9</sup> J. R. Petta, A. C. Johnson, J. M. Taylor, E. A. Laird, A. Yacoby, M. D. Lukin, C. M. Marcus, M. P. Hanson, and A. C. Gossard, *Science* **309**, 2180 (2005)
- <sup>10</sup> R. Hanson, L. P. Kouwenhoven, J. R. Petta, S. Tarucha, and L. M. K. Vandersypen, *Rev. Mod. Phys.* **79**, 1217 (2007)
- <sup>11</sup> B. M. Maune, M. G. Borselli, B. Huang, T. D. Ladd, P. W. Deelman, K. S. Holabird, A. A. Kiselev, I. Alvarado-Rodriguez, R. S. Ross, A. E. Schmitz, M. Sokolich, C. A. Watson, M. F. Gyure, and A. T. Hunter, *Nature* **481**, 344 (2012)
- <sup>12</sup> M. D. Shulman, O. E. Dial, S. P. Harvey, H. Bluhm, V. Umansky, and A. Yacoby, *Science* **336**, 202 (2012)
- <sup>13</sup> Z. Shi, C. B. Simmons, J. R. Prance, J. K. Gamble, T. S. Koh, Y.-P. Shim, X. Hu, D. E. Savage, M. G. Lagally, M. A. Eriksson, M. Friesen, and S. N. Coppersmith, *Phys. Rev. Lett.* **108**, 140503 (2012)
- <sup>14</sup> J. Levy, *Phys. Rev. Lett.* **89**, 147902 (2002)
- <sup>15</sup> H. Bluhm, S. Foletti, I. Neder, M. Rudner, D. Mahalu, V. Umansky, and A. Yacoby, *Nature Physics* **7**, 109 (2011)
- <sup>16</sup> The logical “1” in Ref. 5 contains also the triplet with spin projection  $-1$ . For our purposes we need only the orbital structure of the qubit to obtain the charge density, thus we can disregard the detailed spin structure.
- <sup>17</sup> A. Barenco, C. H. Bennett, R. Cleve, D. P. DiVincenzo, N. Margolus, P. Shor, T. Sleator, J. A. Smolin, and H. Weinfurter, *Phys. Rev. A* **52**, 3457 (1995)
- <sup>18</sup> J. C.-E. Sten, *Journal of Electrostatics* **64**, 647 (2006)
- <sup>19</sup> G. Burkard, D. Loss, and D. P. DiVincenzo, *Phys. Rev. B* **59**, 2070 (1999)
- <sup>20</sup> N. Schuch and J. Siewert, *Phys. Rev. A* **67**, 032301 (2003)
- <sup>21</sup> T. Hiltunen, H. Bluhm, S. Mehl, and A. Harju, *Phys. Rev. B* **91**, 075301 (2015)
- <sup>22</sup> R. Winkler, *Spin-Orbit Coupling Effects in Two-Dimensional Electron and Hole Systems* (Springer Berlin Heidelberg, 2003) pp. 201–206
- <sup>23</sup> M. Trif, V. Golovach, and D. Loss, *Phys. Rev. B* **75**, 085307 (2007)
- <sup>24</sup> It might be surprising why we can write the result again as an addition of only the first excited states, given the fact that the SW transformation includes all excited states. This is so because of the specific form of the SHO eigenfunctions, which leads to a finite coupling through the Rashba SOI only for the states with adjacent energies and all other contributions are zero because of orthogonality.
- <sup>25</sup> W. Knap, C. Skierbiszewski, A. Zduniak, E. Litwin-Staszewska, D. Bertho, F. Kobbi, J. L. Robert, G. E. Pikus, F. G. Pikus, S. V. Iordanskii, V. Mosser, K. Zekentes, and Y. B. Lyanda-Geller, *Phys. Rev. B* **53**, 3912 (1996)
- <sup>26</sup> C. Tahan and R. Joynt, *Phys. Rev. B* **71**, 075315 (2005)
- <sup>27</sup> H. Malissa, W. Jantsch, M. Mühlberger, F. Schäffler, Z. Wilamowski, M. Draxler, and P. Bauer, *Acta Physica Polonica A* **105**, 585 (2004)
- <sup>28</sup> T. Takakura, M. Pioro-Ladrière, T. Obata, Y.-S. Shin, R. Brunner, K. Yoshida, T. Taniyama, and S. Tarucha, *Applied Physics Letters* **97**, 212104 (2010)
- <sup>29</sup> B. Braunecker, G. I. Japaridze, J. Klinovaja, and D. Loss, *Phys. Rev. B* **82**, 045127 (2010)
- <sup>30</sup> C. H. Yang, A. Rossi, R. Ruskov, N. S. Lai, F. A. Mohiyaddin, S. Lee, C. Tahan, G. Klimeck, A. Morello, and A. S. Dzurak, *Nat. Commun.* **4** (2013)
- <sup>31</sup> K. Takashina, Y. Ono, A. Fujiwara, Y. Takahashi, and Y. Hirayama, *Phys. Rev. Lett.* **96**, 236801 (2006)